**AAC Accepted Manuscript Posted Online 5 March 2018**
**Antimicrob. Agents Chemother. doi:10.1128/AAC.02419-17**
**Copyright © 2018 American Society for Microbiology. All Rights Reserved.**

AAC

# **Title:** Topical treatment for cutaneous leishmaniasis – dermato-pharmacokinetic led optimisation of benzoxaboroles

**Journal suggestion:** Antimicrobial agents and chemotherapy

**Byline:** Katrien Van Bocxlaer[1], Eric Gaukel[2], Deirdre Hauser[2], Seong Hee Park[2], Sara Schock[2], Vanessa Yardley[1], Ryan Randolph[2], Jacob J. Plattner[3], Tejal Merchant[3], Simon L. Croft[1], Robert T. Jacobs[3] and Stephen A. Wring[2]

**Affiliations:**

[1] London School of Hygiene & Tropical Medicine, Faculty of Infections and Tropical Diseases, Keppel Street, London WC1E 7HT, United Kingdom

[2] SCYNEXIS Inc., Research Triangle Park, North Carolina, USA

[3] Anacor Pharmaceuticals, Inc., Palo Alto, California, USA

**Corresponding author:** Simon L. Croft, Faculty of Infectious and Tropical Diseases, London School of Hygiene & Tropical Medicine, Keppel Street, London WC1E 7HT, United Kingdom; simon.croft@lshtm.ac.uk, phone: +44 (0)20 7927 2601, fax: +44 (0)20 7927 2739

AAC

## Abstract

Cutaneous leishmaniasis (CL) is caused by several species of the protozoan parasite *Leishmania* – affecting an estimated 10 million people worldwide. Previously reported strategies for the development of topical CL treatments have focussed primarily on drug permeation and formulation optimisation as the means to increase treatment efficacy.

Our approach aims to identify compounds with anti-leishmanial activity and properties consistent with topical administration. Of the test compounds, five benzoxaboroles showed potent activity ($EC_{50}$< 5 µM) against intracellular amastigotes of at least one *Leishmania* species and acceptable activity (20 µM< $EC_{50}$ <30 µM) against two more species. Benzoxaborole compounds were further prioritised based upon the *in vitro* evaluation of progression criteria related to skin permeation such as the partition coefficient and solubility. An MDCK-MDR1 assay showed overall good permeability and no significant interaction with the P-glycoprotein transporter for all substrates except LSH002 and LSH031. The benzoxaboroles were degraded, to some extent, by skin enzymes but have superior stability than para-hydroxybenzoate compounds that are known skin esterase substrates. Permeation evaluation through reconstructed human epidermis showed LSH002 to be most permeable followed by LSH003 and LSH001. Skin disposition studies following finite drug formulation application to mouse skin demonstrated the highest permeation for LSH001 followed by LSH003 and LSH002 with a significantly higher amount of LSH001 retained in skin compared to other compounds.

Finally, the efficacy of the leads (LSH001, LSH002 and LSH003) was tested *in vivo* against *Leishmania major*. LSH001 suppressed lesion growth upon topical application and LSH003

reduced the lesion size following oral administration.

## Introduction

The leishmaniases are a group of neglected tropical diseases, caused by the obligate intracellular protozoan parasite *Leishmania* that mainly occurs in low- to middle-income countries. Leishmaniasis is endemic in 98 countries over five continents placing 350 million people at risk of infection (1). Over 17 different *Leishmania* species can cause a variety of clinical symptoms that depend both on host and parasite related factors.

The most common form CL is widely distributed, with 70-75% of the estimated cases occurring in Afghanistan, Algeria, Colombia, Brazil, Iran, Syria, Ethiopia, North Sudan, Costa Rica and Peru (1) and continues to spread due to environmental changes such as deforestation, travel, emigration and agricultural practice (2-5). In its simplest form, CL presents as a single local skin lesion that tends to heal spontaneously over a period of 3-18 months leaving scars (6). However, a range of clinical manifestations of variable severity are observed in patients that do not achieve spontaneous clearance of the parasite. These manifestations include nodules, ulcers and plaques depending upon the *Leishmania* species causing the infection and the status of host immune system (7). Immediate treatment is vital to expedite healing, reduce scar formation, prevent relapse or to prevent parasite dissemination.

Drugs commonly utilised to treat CL such as pentavalent antimonials, miltefosine, amphotericin B and paromomycin are limited by parenteral drug administration, toxicity, variable efficacy and cost. Over the past decade, despite efforts in screening and drug discovery to identify new chemical series for visceral leishmaniasis (8, 9), only a few novel chemical classes have been explored for CL. Instead, research mainly focussed on repurposing existing drugs or novel

AAC

formulation strategies. For example amphotericin B, currently approved for parenteral delivery has been evaluated for topical delivery in formulations (10) including lipid nano-carriers (11, 12), nano-emulsions (13) or cyclodextrin complexes (14). Similarly, the anti-leishmanial drug paromomycin was formulated in conventional topical vehicles (15-18) and in novel delivery systems including liposomes (19) in an attempt to increase skin permeation. However, the physicochemical properties of both drugs are unfavourable for skin permeation and the reformulation strategies for these compounds have met with limited success.

To enable the further development of treatments for CL we previously characterised how *Leishmania* infection impacts the permeability of the skin barrier and how this might influence topical drug delivery during the acute phase of the treatment (20). These studies have demonstrated that the skin barrier is compromised during the nodular stage of CL suggesting a weaker barrier to dermal delivery.

Besides identifying disease related changes to drug delivery, the identification of drug compounds that are active against a broad range of *Leishmania* parasites is also key (21). Benzoxaborole compounds, characterised by the boron atom incorporated in a ring system fused to an aromatic ring (Table 1), have previously shown activity against bacteria, fungi and protozoans such as *Trypanosoma brucei* and *Plasmodium falciparum* (22-27). Phenotypic screenings of a library of benzoxaboroles identified *in vitro* and *in vivo* activity of benzoxaboroles 6-carboxamides against *T. brucei* and *T.cruzi,* the causative agents of human African trypanosomiasis (HAT) and Chagas disease (22, 28), respectively. Additionally, more than 2000 compounds were evaluated against *L. donovani* amastigotes in THP-1 cells to identify

AAC

drugs to treat visceral leishmaniasis and resulted in several hits with micromolar activity (DNDi funded work, unpublished data).

Here we describe an approach for the rational pre-clinical selection of candidate molecules for CL (Figure 1 (A)), using a series of benzoxaboroles that were found to (i) demonstrate activity against a selection of *Leishmania* species (ii) have the ability to permeate skin and (iii) were appropriately distributed in various skin layers (Figure 1 (B)).

## ***Materials and Methods***

### **Materials**

Compounds were synthesised by Anacor Pharmaceuticals Inc. and SCYNEXIS Inc. (Research Triangle Park, NC) and were of >95% purity as determined by HPLC, LC-MS and $^1$H-NMR analyses. Stock solutions (1 mM) were prepared in dimethyl sulfoxide (DMSO) for use in the *in vitro* experiments. HPLC grade solvents were purchased from Fisher Scientific (Pittsburgh, PA). Formic acid (≥98% purity, Fluka), caffeine, testosterone, 1-octanol, high grade vacuum silicone grease (Dow Corning) were acquired from Sigma-Aldrich (St. Louis, MO). Ammonium formate (99% purity, Alpha Aesar) was purchased from VWR International, LLC (West Chester, PA). Miglyol 840 (propylene glycol dicaprylate / dicaprate) was obtained from Sasol Germany GmbH (Witten, Germany). Phosphate buffered saline (PBS) was supplied by Gibco (Invitrogen Corporation, Carlsbad, CA) as well as the Dulbecco's modification of Eagle's medium with GlutaMAX, the trypsin-EDTA and the Fetal Bovine Serum. Penicillin-Streptomycin solution, Hank's balanced salt solution and HEPES buffer were obtained from Sigma Aldrich.

### **Mice**

Female BALB/c mice (6-8 weeks old) were purchased from Charles River (Margate, UK) and housed in a controlled environment of 55% relative humidity and 26°C. Tap water and a standard laboratory diet were provided ad libitum. All *in vivo* experiments were carried out under license (PPL 70/8207) at the London School of Hygiene & Tropical Medicine (LSHTM) after discussion with the veterinarian, clearance through the LSHTM Animal Welfare and Ethical Review Board and according to UK Home Office regulations.

### Parasite and cell maintenance

*L. major* (MHOM/SA/85/JISH118); *L. panamensis* (MHOM/PA/67/BOYNTON); *L. aethiopica* (MHOM/ET/84/KH); *L. mexicana* (MNYC/ BZ/62/M379) and *L. tropica* (MHOM/IR/2013/HTD4) were routinely passaged through BALB/c mice, and low passage number promastigotes (typically below passage number 3) were used for the assays. All promastigotes, except for *L. panamensis* and *L. aethiopica*, were maintained in Schneider's insect medium (Sigma Aldrich, UK) supplemented with 10% heat inactivated foetal calf serum (HiFCS) (Harlan, UK) at 26°C. M199 medium supplemented with 10% HiFCS was used for the latter two strains.

MDCKII-hMDR1 cells (Netherlands Cancer Institute, Amsterdam, Netherlands) were maintained in Dulbecco's Modified Eagles Medium (DMEM) and KB cells in RPMI-1640 medium supplemented with L-glutamine and 10% HiFCS. Both human-derived cell lines were left in an incubator at 37ºC and 5% $CO_2$ and passaged to new medium once a week (1/10 ratio).

### *In vitro* anti-leishmanial activity

Mouse peritoneal macrophages (PEM) were isolated from CD-1 mice (Charles River, Margate, UK) by abdominal lavage with RPMI-1640 medium containing 1% penicillin and streptomycin. The collected cells were washed, re-suspended and seeded in 16-well Lab-Tek™ slide in RPMI-1640 supplemented with 10% HiFCS at a density of $4x10^4$ per well. After 24 hours incubation at 37°C and 5% $CO_2$/95% air mixture, the adhered PEMs were infected with stationary phase promastigotes at a ratio of 3 (for *L. tropica* and *L. major*) or 5 (for *L. mexicana*, *L. aethiopica* and *L. panamensis*) promastigotes to 1 macrophage and maintained at 34°C in a 5% $CO_2$/95% air

AAC

mixture. These inoculum ratios were chosen to achieve at least 75% infection of untreated control macrophages after 72 hours of incubation.

After 24 hours, the cultures were washed to remove extracellular promastigotes and one slide was fixed with methanol and stained with Giemsa to determine the initial level of infection. If a sufficient level of infection was obtained, experimental drug solutions over a range of 30, 10, 3 and 1 µM were added in quadruplicate at each concentration. Amphotericin B (Fungizone®) and miltefosine were included as control drugs. After 72 hours incubation, all slides were methanol-fixed and Giemsa-stained.

The percentage inhibition was determined by microscopically (400x magnification) counting the infected macrophages in drug treated cultures compared to untreated cultures. The Hill coefficient, $EC_{50}$ and $EC_{90}$ values were calculated by non-linear sigmoidal curve fitting (variable slope) using Prism Software (GraphPad, Surrey, UK).

### *In vitro* ADME studies–general pharmacokinetic predictions

The following descriptors of the test compounds: molecular weight, aqueous solubility and number of H-bond donors and acceptors present were calculated using ChemBioDraw Ultra 13.0 (PerkinElmer, Waltham, MA).

*Distribution coefficient*. The octanol phase was left to saturate with PBS (pH7.4) on a shaking plate at 32°C for 48 hours. The test compounds were then dissolved in the 1-octanol at a concentration of 1 µg/ml and left to equilibrate with an equal volume of PBS on a shaking plate at 32°C for 48 hours. The 1 ug/ml concentration was selected such that the amount of the

AAC

candidate drug in each phase did not exceed 10% of the solubility limit of that compound. Aliquots of each phase were taken and diluted in mobile phase followed by LC-MS/MS analysis. Each experiment was conducted in triplicate. The distribution coefficient was calculated as shown in Equation 1:

$$\log \mathrm{D}\ (\mathrm{pH}\ 7.4) = \log\left[\frac{[\mathrm{solute}]_{\mathrm{oct}}}{[\mathrm{solute}]_{\mathrm{pbs}}^{\mathrm{ion}} + [\mathrm{solute}]_{\mathrm{pbs}}^{\mathrm{neutral}}}\right] \qquad \text{Equation 1}$$

*In vitro prediction of permeability and Pgp-mediated efflux transport.* MDCK-MDR1 cells were seeded in the apical chamber of a 12-well Transwell® plate (Corning Inc., Lowell, MA) at a density of 6.6x10$^6$ cells/well and 1.5 mL of medium was applied in the basolateral chamber. After 24 hours, non-adhered cells were washed away and new medium was applied to both chambers. The cells were incubated for an additional 48 hours at 37°C to form confluent monolayers.

Prior to the addition of the test compounds, the cell culture medium was removed and replaced with transport medium consisting of Hanks's balanced salt solution with 24 mM of glucose and 24 mM of HEPES buffer. The integrity of the monolayers was assured by measuring the trans-epithelial resistance (TEER) for each insert (TEER > 160 Ω cm$^2$). Assays were performed in triplicate by adding 3 µM drug solutions (1 mM DMSO stock solutions diluted in transport medium) in the absence or presence of 2 µM GF918 (a potent Pgp inhibitor (29)) in the transport buffer of the apical chamber. The comparator controls propranolol and amprenavir for transcellular transport and Pgp efflux respectively were included in each assay. The Transwell® plates were incubated on a shaking plate (160 rpm) at 37°C and 5% $CO_2$ for 1 hour. After incubation, aliquots from both chambers were removed for analysis by LC-MS/MS.

Values for mass balance, apparent permeability for the apical to the basolateral side ($P_{app}$) (Equation 2), apparent permeability value for the apical to the basolateral in presence of GF+918 ($P_{app+GF918}$), and the absorption quotient (AQ) (Equation 3) were calculated for each compound (30-32). Test compounds with an AQ ≤ 0.3 were considered non-Pgp substrates, while AQ > 0.3 were considered Pgp substrates (31, 32). Acceptance criterion for mass balance was 70–120%.

$$\boldsymbol{P_{app}} = \frac{\boldsymbol{dQ/dt}}{\boldsymbol{C_0 \times A}} \qquad \text{EQUATION 2}$$

$$\boldsymbol{AQ} = \frac{\boldsymbol{P_{app+\,GF918} - P_{app}}}{\boldsymbol{P_{app+\,GF918}}} \qquad \text{EQUATION 3}$$

### Analysis of test compounds in biological samples

*Skin tissue homogenisation.* For the preparation of the skin homogenates, 20 ml of ice-cold Dulbecco's modified PBS (pH 7.4) was added to fine pieces of approximately 2 g of shaved dorsal full-thickness BALB/c mouse skin (Bioreclamation LLC., Westbury, NY). The tissue suspension was homogenized using an OMNI probe homogenizer (Kennesaw, GA) and centrifuged for 10 minutes at 800g to sediment cellular residue. The protein content of the supernatant was determined using the Pierce BCA protein assay kit (Pierce, Rockford, IL) and adjusted to 2.5 mg/ml. The supernatant was stored at approximately -80°C until use.

*High performance liquid chromatography with tandem mass spectrometry (LC-MS/MS).* Sample analysis was performed by LC-MS/MS. The instrumentation consisted of a CTC Pal Autosampler (Leap Technologies, Carrboro, NC), two Agilent 1100 series pumps (Agilent Technologies Inc., Santa Clara, CA), a CH-30 column heater (Eppendorf, Hauppauge, NY) and an API-3000 triple quadrupole mass spectrometer (Applied Biosystems, Foster City, CA) equipped with a turbo-ion electrospray interface for detection. Chromatography was performed on a Luna C18 reversed-phase column (50 x 2 mm; 3 µm) from Phenomenex (Torrance, CA) protected by a matched phase guard column. The mass spectrometer and peripheral devices were controlled using Analyst® Software version 1.4.2 (Applied Biosystems, Foster City, CA). The mobile phase used to elute the compounds consisted of 5 mM ammonium formate and 0.1% (v/v) formic acid in water (A) and 5 mM ammonium formate and 0.1% (v/v) formic acid in methanol (B). The samples were introduced on the column using 90% A at a flow rate of 600 followed by a step gradient to 90% B between 0.5 and 1min. For analytical chromatography, a linear gradient of 10% A was maintained for 2min after which the mobile phase was switched back to 90% A. This mobile phase composition was maintained till the end of the run (3.5min). Test compounds eluted between 2-3 min.

### ***In vitro*** **stability and disposition in skin homogenates**

*Stability in skin homogenates.* The stability of the compounds was measured at protein concentrations of 2.5 mg/ml. Each compound (10 µM) was incubated in mouse skin homogenate on a shaking plate at 32°C. An aliquot of the incubation mixture was collected at 0, 10, 20, 30 minutes, 1 hour and 2 hours and quenched with 4 volumes of ice-cold methanol containing 0.1% formic acid. Samples were centrifuged at 3000xg for 10 minutes at 15°C, and the obtained supernatant was analysed for the test compound by LC-MS/MS. Ethyl- and

AAC

propylparaben, ester compounds known to undergo degradation due to enzymatic hydrolysis to yield hydroxybenzoic acid were included as positive controls.

*Skin tissue binding.* Rapid equilibrium dialysis (RED) devices (Pierce, Rockford, IL) in plate format were used to determine the drug binding to the skin homogenate supernatant. A day prior to the experiment, the Teflon plate was washed with 30% ethanol and rinsed twice with deionized water before leaving it to dry. On the day of the experiment, skin supernatant was thawed and the test compound was added to a final concentration of 10 µM. Samples of fortified skin tissue homogenate (300µl) were added to the sample chambers of the RED devices and PBS (500µl) (Pierce, Rockford, IL) was added to each buffer chamber. Plates were incubated on a shaking plate at 32°C for 2 hours. Aliquots of both phases were collected and treated with 4 volumes of ice-cold methanol with 0.1% of formic acid to precipitate proteins. Treated sample aliquots were centrifuged at 3000xg and 15°C for 10 minutes. The resulting supernatants were assayed for the parent drug concentration by LC-MS/MS.

*In vitro prediction of skin permeability.* The EpiDerm™ Skin Model EPI-606-X was obtained from MatTek Corporation (Ashland, MA, USA). The EPI-606-X model is characterised by an enhanced barrier function and was specifically designed to conduct permeability assays. Upon receipt, the skin tissue (lot 17860) was stored overnight at 2-8°C. On the day of the experiment, the skin inserts were transferred to a 6-well plate containing 2ml of Dulbecco's modified PBS and left to acclimatise on a heated shaking plate. The temperature was set at 36.6°C which corresponded to a skin temperature of 32°C.

Due to a low water solubility, the test compounds were prepared in an ethanol/ Miglyol 840 (1:9) vehicle - a solution that has been used for permeation studies with poorly soluble drugs (33). After 1 hour, 1.14 ml of a 100 µg/ml donor solution was applied on the model skin using a positive displacement pipette. The plates were left to incubate with gentle shaking at 95 rpm. Caffeine (log P=-0.08) and testosterone (log P=3.32) were included as control comparator compounds in each assay run. Each control was evaluated at the same concentration as the test compounds. Testosterone, representing a hydrophobic control, was formulated in the ethanol/Myglyol vehicle, and caffeine representing a hydrophilic control, was prepared in Dulbecco's modified PBS. Aliquots were removed from the receiver fluid of each chamber and replaced with fresh PBS at regular time points over the course of 6 hours incubation. The samples were assayed for test compound by LC-MS/MS. The permeation of each compound was evaluated in triplicate. Statistical analyses were performed using SPSS software version 19.0.

### Skin disposition

*In vitro permeation prediction using full-thickness BALB/c mouse. In vitro* permeation studies were conducted in a semi-automated system comprising 6 water-jacketed, static, vertical type Franz diffusion cells (FDC) from Logan instruments Ltd. (Somerset, NJ). The permeation studies had two objectives (Table 2). The first objective was to compare the permeation of the test compounds through BALB/c mouse skin to the permeability determined by means of the RHE assay. Therefore, the experimental conditions were held consistent to those employed for the RHE assay. The second objective was to compare the permeation of the test compounds using

AAC

the formulation conditions that would be used for topical dose administration in the murine model of CL. This *in vivo* study required a low application volume and a 1% (w/v) drug formulation.

For FDC studies, female BALB/c mouse skin was obtained from Bioreclamation IVT (Westbury, NY, USA) and stored at -80°C. On the day of each study skin was thawed and hair removed by careful clipping to avoid skin damage. Excess fat and muscle tissue was removed with the aid of a scalpel. Discs of skin approximately 2.5cm in diameter were cut and mounted between the donor and receptor compartment of each FDC and kept in place by the use of a clamp. Vacuum silicone grease was applied to seal gaps and prevent leakage. The cells were left to equilibrate until the skin temperature stabilised at 32°C.

The donor and receptor solutions were prepared as described above. Receptor fluid samples were taken at time intervals over a period of 6 hours. Each test compound was tested in triplicate. Statistical analysis was performed using SPSS software version 19.0.

*Mass balance during FDC studies.* Mass balance study was conducted using the formulations and experimental conditions intended for evaluation in the murine model of CL. The amount of drug that did not permeate into or through the skin (unabsorbed donor fraction) was obtained by gently swabbing the skin surface with a cotton bud at the end of the permeation experiment. This was repeated a second time. The cotton buds were placed in a tube with 1ml of MeOH/PBS (70:30) and left overnight on a shaker (800 rpm). An aliquot of the extraction fluid was analysed by LC-MS/MS.

The Franz diffusion cells were dismantled and the mouse skin was removed and placed in a vial. Three rounds of extraction with 1ml of MeOH-PBS (7:3) were conducted. At each time, the vial was left to shake overnight before analysis by LC-MS/MS to extract the amount of drug that permeated into the skin. Acceptable mass balance was 80-120% representing the total compound measured in the unabsorbed donor fraction, methanolic skin extracts, and the samples of receptor chamber fluid. Statistical analyses were performed using SPSS software version 19.0.

**Efficacy in a murine model of cutaneous leishmaniasis**

*Drugs and formulation preparation.* AmBisome®, a liposomal formulation of amphotericin B for injection was kindly provided by DNDi (Geneva) and prepared according to manufacturer's recommendations. Briefly, AmBisome® powder was reconstituted with 12ml of cold sterile ultra-high purity grade water (>18 MΩ.cm, MilliQ, Hertfordshire) to produce a 4 mg/ml amphotericin B liposomal suspension. This suspension was vigorously shaken and incubated at 65°C for 10 minutes after which it was allowed to cool to room temperature. This dispersion was diluted with sterile 5% dextrose solution (w/v) to obtain a final suspension of 0.5mg of amphotericin B/ml. Every other day up to 5 doses, 200ul of this formulation was administered by bolus intravenous injection into a lateral tail vein. Leshcutan® ointment, containing 12% of paromomycin and 15% methylbenzethoniumchloride (Teva, Israel) was purchased from Israelpharm.com and 0.1ml of a 1ml syringe was applied and gently spread over the nodule twice daily for 10 days.

AAC

The experimental topical formulations containing compounds LSH001, LSH002 and LSH003 respectively were prepared 24 hours prior to the start of dosing. To allow maximal permeation, each test compound was applied as a saturated solution. An excess amount of the test compound was added to a 1:1 (v/v) mixture of propylene glycol (PG) and ethanol (Ethanol). The mixture was left to stir overnight after which it was centrifuged at 15,668 x g for 15 minutes. The supernatant, i.e. a saturated solution, was pipetted into a clean vial and 50ul was applied to each mouse twice a day for 10 days (Table 3).

The standard suspension vehicle used to prepare the oral formulations was prepared by weighing and adding each component (0.5% (w/v) carboxymethylcellulose, 0.5% (v/v) benzyl alcohol, 0.4% Tween 80 (v/v) in a 0.9% (v/v) NaCl solution) into a clean glass vial. The mixture was left to stir overnight at room temperature prior to sterilisation by autoclaving. The experimental oral formulations containing either LSH001, LSH002 or LSH003 in the vehicle were prepared by adding the appropriate amount of test compound to the vehicle in order to obtain a final concentration of 2.5mg/ml. The suspension was sonicated for 30 minutes and was administered orally twice a day for 10 days. All formulations, including the AmBisome and topical formulations were stored at 4˚C throughout the experiment.

*Experimental CL model.* Sixty female BALB/c mice (6-8 weeks old; Charles River Ltd., UK) were shaved on the rump above the tail and one day later, injected with 2x$10^7$ stationary phase *L. major* JISH118 promastigotes (200 µl) subcutaneously on the rump above the tail. Approximately 7 days post infection, small nodules were visible. The nodule size was recorded daily and when they reached an average diameter of 4.8 mm (±0.8), the mice were randomly

AAC

allocated in groups of 6 and drug administration was started. Formulations were administered over a period of 10 days. Untreated and topical vehicle only control groups were included.

Treatment efficacy was evaluated by lesion size progression, measuring the lesion diameter in 2 dimensions on a daily basis using digital callipers (Jencons Scientific Ltd., UK). The average diameter was plotted as a function of time. Statistical analyses of differences between the average lesion diameter between groups on the last day of treatment was performed using one-way ANOVA with post-hoc Tukey test (SPSS software version 19.0). Three days after the end of treatment, the mice were sacrificed and the lesion was excised and stored at -80°C until the parasite load was quantified using real-time qPCR. Statistical differences in the average parasite numbers between different groups were analysed using one-way ANOVA with Tukey post-hoc test (SPSS software, version 19.0).

*Quantification of the parasite load in a CL lesion.* On the day of extraction the samples of lesion tissue were defrosted and cut into 2 approximately equal samples. One half was weighed and cut into fine pieces with a surgical blade before placing in a microcentrifuge tube. The proteinase K and lysis buffer were added to the tube and samples were incubated at 56°C until a homogeneous mixture was obtained. The DNA of 200ul of this homogenate was then extracted using the DNeasy® blood and tissue kit (Qiagen) and eluted in the same volume. The purity and concentration of DNA was analysed using the NanoDrop™ ND1000 spectrophotometer (Thermo Fisher Scientific).

The primer pair and probe, previously designed and validated by Van Der Meide et al (34) targeted a 170-bp region in the *Leishmania* 18S ribosomal gene and are specific for all

AAC

*Leishmania* species. The respective sequences are shown in Table 4. Conventional PCR was performed to confirm the presence of PCR product of the correct size and to verify primer efficacy. 1µl of a 1/100 dilution of the DNA extract was amplified in a final volume of 10µl containing 2µl of KAPA 2G buffer (Kapa Biosystems, Wilmington, MA) and primers at a concentration of 0.4µM. The samples were run in a G-Storm GS4 machine (Somerset, UK). The amplification cycle started with a denaturation step at 95°C for 3 minutes followed by 40 cycles of 95°C for 15s, 60°C for 1 minute and 72°C for 30 seconds with a final extension of 72°C for 30 seconds. Each run contained a negative sample whereby the extracted DNA was replaced by UHP water. The PCR products were separated on a 3% agarose gel stained with ethidium bromide and visualised under UV light. A 100-bp DNA ladder was run in parallel with the samples.

The parasite load was determined by means of quantitative PCR. For the amplification reaction, 2µl of a 1/100 diluted DNA sample was added to 8µl mix containing 5µl KAPA Probe Fast qPCR master mix (2x) (Kapa Biosystems, Wilmington, MA), 0.4 µM of each primer and 0.25µM of the appropriate probe. The tubes were placed in the 72 sample rotor of the instrument (Rotor Gene 3000, Qiagen) and the reaction with the following conditions was initiated: 95°C for 3 minutes followed by 40 cycles of 95°C for 3 seconds and 60°C for 30 seconds. Each run contained a standard curve, a no-template-control and a negative control.

AAC

## *Results*

### *Structures of the compounds*

Benzoxaborole compounds from 4 different chemical classes that had shown anti-parasitic activity in the *P. falciparum*, *T. brucei*, *T. cruzi* or *L. donovani* screens were selected from the library for screening against CL causing species. Some of the subclasses tested are shown in Table 1 and include benzoxaborole 6-carboxamides (D), benzoxaborole-5-carboxamides (B), pyrazole 6-carboxamides (C) and benzoxaborininols (E) in which the 5-ring containing the boron atom is replaced by a 6-ring structure.

### *In vitro* **anti-leishmanial activity**

Twenty-five compounds were screened against intracellular amastigotes. LSH001, LSH003, LSH023, LSH024 and LSH025 were the only five compounds that showed activity against at least one Old World (*L. major*, *L. tropica* and *L. aethiopica*) and one New World (*L. mexicana* and *L. panamensis*) species with an $EC_{50}$ value below 30 µM (Table 5). These five test compounds were most active against *L. tropica* with an $EC_{50}$ value below 5 µM followed by *L. major* with $EC_{50}$ values in the same range. *L. mexicana* was the least susceptible species with $EC_{50}$ values ranging from 9 to 22 µM. For most tested compounds, the $EC_{50}$ value against *L. mexicana* was higher than 30 µM, the highest concentration tested suggesting low activity of the compound.

Amphotericin B, included as positive control, had a high activity with $EC_{50}$ values ranging from 0.049 to 0.685 µM, indicating a tenfold difference in sensitivity between *L. major*/*L. tropica* and *L. mexicana.* Miltefosine, the other control drug, was less active than amphotericin B with $EC_{50}$ values ranging from 7 to 45 µM and 10 to 35 µM respectively.

At this stage, it was decided to advance all compounds with potent ($EC_{50}$ <5uM) and/or moderate activity (5uM<$EC_{50}$<25uM) against at least one Old World and one New World *Leishmania* species. Eight compounds (LSH026-034) with promising activity against other *Leishmania* species (DNDi, unpublished data) were also included in further assays.

### Physicochemical properties

An initial computational screening of the test compounds was conducted to evaluate permeation related physicochemical properties i.e. the molecular weight, the presence of H-bond donors or acceptors and the aqueous solubility. The partition coefficient was determined experimentally. It was found that the benzoxaborole test compounds had appropriate physicochemical profiles for skin permeation (Table 6), i.e. a molecular weight below 500 g/mol, a log D (at pH 7.4) between 1-3 (except for LSH002 (logD = 0.44) and LSH032 (logD = 0.88)) and no more than 2 H-bond donor groups.

### Intrinsic permeability

The MDCK-MDR1 assay was performed to identify P-glycoprotein (Pgp) substrate and to evaluate passive permeability of the test compounds across simple epithelia such as that of the intestine (35). The test compounds generally demonstrated high passive permeability (Table 7) in the assay with values ranging from 247-688 nm/s (32) except for compound LSH002 that showed a low intrinsic permeability of 32.5 nm/s. Further, only one compound (LSH002; AQ value: 0.492) exceeded the cut-off value (>0.3) for absorptive quotient indicating it was a potential substrate for the efflux transporter Pgp. For comparison, Amprenavir, the positive control included as a known Pgp substrate afforded an AQ value of 0.846. Interestingly, the

AAC

most active compounds during in vitro susceptibility studies all showed permeability values above 300 nm/s and were no Pgp substrates.

Previous research suggested an enhanced permeability of hydrophilic compounds in *Leishmania*-infected skin (20). Compounds LSH002 and LSH032 were therefore included in further assays despite their less favourable physicochemical properties and/or intrinsic permeability.

### Dermal stability, binding and permeability

*Stability in skin supernatant.* An initial rapid drug degradation of the test compounds was observed in skin supernatant (Figure 2) during the first 30 minutes, followed by slower drug metabolism. After two hours, compound recovery was 25 to 60% with LSH001, 002, 024, 025, 028, 031, 032, 034 being moderately stable (% remaining: 25-44) and LSH003, 023, 026, 027, 029, 030, 033, 034 being most stable with 45-75% test compound remaining. The two paraben compounds, ethyl and propyl paraben, known substrates for skin esterases, were observed to break down very quickly in presence of the skin supernatant. The recovery of these labile compounds was 10.9 and 0% respectively after 2 hours of incubation.

*Drug binding to skin components.* A binding assay showed large variations in unbound fractions among the benzoxaboroles; unbound fractions from 34% to 92% were observed (Table 8). Only 2 compounds had a high free fraction of 85% or more comprising LSH001 and LSH026. The majority of the compounds has a free fraction between 50 and 85% and finally LSH003 and LSH023 with the lowest free fractions of 44 and 34% respectively.

*RHE permeability.* RHE was used to evaluate the passive permeability of the test compounds across multiple layered membranes more representative of skin. The permeation of LSH002 was statistically significant higher compared to LSH001, LSH029 and LSH033 (one-way ANOVA, $p<0.05$). As anticipated, the high permeability hydrophilic control caffeine showed the highest permeation, which was significantly higher when compared to all the test compounds and testosterone (lower permeability, hydrophobic control) after 6 hours (one-way ANOVA; $p < 0.05$). When ranking the cumulative amount permeated over 6 hours, the rank order from high to low was as follows: caffeine > LSH002 > LSH003 > LSH023 > testosterone > LSH024 > LSH033 > LSH001 > LSH029.

Both caffeine and LSH002 are more hydrophilic compounds as indicated by their low log D of -0.08 and 0.44, respectively. The vehicle in which all drugs were applied was ethanol-Miglyol 840 (1:9). LSH002 even though in solution, might have been closer to saturation exhibiting a higher thermodynamic activity compared to the other test compounds with a higher log D. The higher permeation exhibited by LSH002 could also involve the higher affinity of this compound for the RHE compared to the lipophilic vehicle thereby stimulating its preferential partitioning into the membrane.

Based on the overall data set collected, it was decided to select three compounds (LSH001, LSH002 and LSH003) for further study. LSH001 was included because it showed potent anti-leishmanial activity and was representative of a lipophilic compound, despite lower permeability, that may prove helpful for formulation and skin disposition. LSH002 was included due to its higher solubility in water and hence a control for disposition in the skin permeation

AAC

assay and LSH003 was selected because it was active against the 5 *Leishmania* species tested and it was ranked second with regards flux in the permeation assay.

### Dermal disposition

The objective of the first permeation study in mouse skin was to verify the rank order of the three selected compounds and compare them with the results obtained from the previous permeation experiment where a RHE model was used (Table 9). Therefore, the experimental conditions and drug formulations were similar to the RHE experiment. The results are shown in Figure 3 and indicate that the rank order LSH002 > LSH003 > LSH001 is maintained when using BALB/c mouse skin instead of the RHE membrane. Furthermore, the permeation of LSH002 through BALB/c mouse skin was significantly higher compared to LSH001, LSH003 and testosterone (one-way ANOVA, $p<0.05$).

A second permeation study using BALB/c mouse skin aimed to assess the permeation and skin disposition of the compounds after application of a low volume of a 1% solution of test compound in ethanol-propylene glycol (E-PG) (1:1) solution (28 $\mu L/cm^2$) comparable with the formulation intended for use in the murine CL model. Permeation (Table 8) was statistically higher for LSH001 and LSH003 ($p<0.05$, one-way ANOVA) compared to LSH002. The rank order for flux was LSH001 > LSH003 > LSH002. Of note, in the E-PG formulation the more hydrophobic compounds (LSH001 and LSH003) achieved greater permeation than LSH002. There was no difference observed in the lag time for the different compounds (ANOVA; $p >0.05$).

A skin disposition study (Figure 4) was conducted to compare the amount of test compound that either: remained on the surface of the skin, retained within the dermal layers or had permeated through the skin. Whilst there was no statistical significant difference between the amounts of compounds that had permeated over 24 hours, the amount of LSH001 in the skin was significantly higher in comparison to LSH002 and LSH003 (one-way ANOVA; $p<0.05$). The mass balance for the total compound recovering was 84%, 87% and 114% for LSH001, LSH002 and LSH003, respectively indicating excellent mass balance was achieved for all compounds across the compartments.

### ***In vivo*** **anti-leishmanial activity**

After 10 days of topical application of the three selected compounds to the closed nodules, LSH001 halted the lesion size progression and the lesions in this group were statistically smaller compared to the vehicle control group (One-way ANOVA, $p<0.05$) whereas no lesion size reduction was observed for LSH002 or LSH003 (Figure 5 (A)). The lesion sizes and parasite burden per lesion of the groups 3 days after the last drug administration are shown in Figure 5 (B). The parasite load in the group receiving topical LSH001 is slightly lower than in the other topically treated groups however there is no statistically significant difference (One-way ANOVA, $p>0.05$).

Whilst the primary aim of this work was to investigate the potential of benzoxaboroles for topical treatment for CL, the *in vitro* ADME data suggest good overall permeability. Previous studies of the benzoxaboroles as orally active drugs for HAT suggested good oral bioavailability for this class. Therefore, we administered the three test compounds LH001, LH002 and LH003 orally to CL infected mice. A significant reduction of lesion size was seen for the groups receiving LSH003 by the oral route compared to the relevant control group (One-way ANOVA,

$p<0.05$). This was also reflected in parasite load as the number parasites per lesion was statistically significant lower compared to the untreated control group (One-way ANOVA, $p<0.05$).

For AmBisome®, the positive control, a statistically significant reduction in lesion diameter and parasite load was observed compared to the control group ($p<0.05$) except for the LSH001 topical and LSH003 oral groups ($p>0.05$). This was expected as per previous reports describing a reduction of both lesion size and parasite burden (36).

## *Discussion*

Topical treatment for a dermatological infection limited to the more superficial layers of the skin, offers an attractive alternative to the currently used routes of administration for CL treatment as it (i) allows local drug targeting directly to the infection site, (ii) offers the potential to limit adverse effects, (iii) is not invasive and (iv) is easy to apply by the patient. A systematic approach to the identification of potential lead compounds to progress to clinical trials is still lacking. The goal of this work was to explore a novel approach to identify promising compounds for the treatment of CL.

The benzoxaborole class of anti-parasitics has demonstrated efficacy across multiple parasitic disease targets including the *Leishmania spp*. DNDI-6148 is at the preclinical stage of development for treatment for visceral leishmaniasis (37) and oxaborole SCYX-7158 is now in phase 2 clinical trials  for the treatment of HAT (37). The goal of these programs was to identify orally active treatments of these systemic parasitic infections.

AAC

AAC

For successful therapeutic activity *in vivo* in CL, a drug requires both potent anti-leishmanial activity and an ability to permeate biological membranes in order to reach the *Leishmania* parasites in the dermal layer of the skin, a process that is impacted by both the physicochemical properties of the drug and the route of administration.

Several criteria limit delivery of drugs through the skin; drugs with a molecular weight of < 500 g/mol (38), a partition coefficient between 1 and 3 (39, 40) , a low melting point (< 200$^{o}$C) (41), aqueous solubility >1 mg/ml (42) and less than 2 H-bond donor groups (43) are more likely to permeate. Topically applied drugs also undergo relatively little enzymatic degradation compared to orally administered drugs that need to pass a monolayer of intestinal epithelium and have low hepatic first-pass metabolism before it reaches the blood circulation to allow it to distribute to the skin (40).

Whilst each layer of the skin is a potential hurdle to drug permeation, it is the outer layer of the skin, the stratum corneum, that is a highly restrictive permeability barrier formed of 10-15 layers of dead keratinized cells imbedded in an intercellular lipid mixture organised in bilayers (44, 45). This inherent difference between bio-membranes governs the preferential permeability of certain drugs (40).

Previously reported strategies for developing topical treatments for CL have focussed solely on formulation optimisation as means to increase treatment efficacy, whereas we wish to identify compounds with intrinsic properties consistent with topical administration. To achieve this objective we systematically evaluated physiologically-based pharmacokinetic parameters and aimed to correlate these to the physicochemical properties of the compounds. A diverse set of

AAC

benzoxoboroles associated with good drug-like properties in previous anti-parasitic programs was selected. Compounds were assessed for their likely intrinsic activity against old and new world CL species by measuring the *in vitro* activity against the intracellular amastigote form using a previously reported assay (46).

Dermal drug-like properties were characterised by comparing physicochemical properties, *in vitro* permeability through MDCK, and RHE models and stability in skin homogenate. Subsequently promising compounds were advanced to whole skin permeability, binding and disposition evaluation. This strategy of selection was employed to advance the most promising compounds to the more complex assays. Ultimately, this strategy identified 3 compounds each with unique features for evaluation in a murine model of CL.

Initially, five benzoxaboroles 6-carboxamides showed broad range activity against CL causing species. To complement this intrinsic activity, *in vitro* membrane permeability assays were employed to assess each compound's ability to cross a cellular barrier. Previously, the MDCK-MDR1 Transwell assay was successfully utilised to classify compounds with a potential high permeability across the gut when $P_{app}$ A→B $_{+GF918}$ >50 nm/s (31) or the blood brain barrier when the $P_{app}$ A→B $_{+GF918}$ >150 nm/s and the compound is a non-PgP substrate (47). Whilst for dermal permeation no clear selection criteria were found in literature, our test compounds generally exhibited high permeability with a $P_{app}$ A→B$_{+GF918}$ >200 nm/s, except for LSH002 ($P_{app}$ A→B$_{+GF918}$ = 32.5 nm/s). Furthermore, the MDCK-MDR1 assay allowed us to identify potential substrates of the P-glycoprotein (PgP) efflux transporter (48-50) which is helpful considering that these compounds may suffer reduced fraction absorbed following oral delivery (51, 52) but may also

AAC

demonstrate reduced ability to penetrate macrophages. This is important because *Leishmania* parasites survive and divide inside macrophages meaning that Pgp substrate drugs might potentially be less active compared to drugs that are not Pgp substrates as efflux would attenuate entry into macrophages (53, 54). In fact, reports of inactivity of antimonial drugs against *L. donovani* in patients were linked to upregulation of Pgp transporters in the host cells, leading to low concentrations of drug in the macrophages and thus disease progression (55). In our set of test compounds, only LSH002 showed an absorption quotient higher than 0.3 indicating it potentially is a Pgp subtrate (31).

Moving on from the cellular models of permeation, the permeability of the test compounds was further evaluated in complex RHE that has shown ability to predict dermal permeation (56) allowing us to further rank order our test compounds. The hydrophilic compounds, caffeine and LSH002, showed highest permeation in this model. Caffeine and LSH002 were the most hydrophilic compounds amongst the test compounds as was indicated by their log D value of -0.08 and 0.44 respectively. Hence, LSH002 even though in solution, might have been closer to saturation in the ethanol-Miglyol 840 (1:9) vehicle exhibiting a higher thermodynamic activity compared to the test compounds with a higher log D. The second highest permeation was observed for LSH003 the test compound that also showed good *in vitro* anti-leishmanial activity against all five *spp*. LSH001, also active *in vitro* against all *Leishmania* spp, showed a slightly lower permeation than testosterone the lipophilic control drug.

When evaluating the permeation of these three compounds in BALB/c mouse skin using the same experimental design, the overall permeation and thus flux of the test compounds and

AAC

testosterone were lower compared to the permeation through RHE (one-way ANOVA, $p < 0.05$) (Table 6). Several studies have indicated that RHE is more permeable than animal and human skin (57-59). The rank order of the test compound's permeation through mouse skin was the same as for the RHE (LSH002 > LSH003 > LSH001) and more importantly, the permeation of all test compounds was higher than that of testosterone.

We next explored the metabolic stability of the benzoxaboroles in both liver-based and skin-based assays. Degradation of drugs in the skin has been reported (60-62) with the main site of activity situated in the epidermis (63). We used the supernatant of skin homogenate to determine the drug stability and observed that all benzoxaborole test compounds showed a higher stability compared to the paraben compounds that are known substrates for skin esterases and are therefore expected to breakdown (64). The fraction of parent compound remaining after 2h of incubation was relatively similar for all compounds ranging from approximately 30 to 60%. The skin homogenate was prepared using full-thickness BALB/c mouse skin as opposed to epidermal membranes alone. Epidermal membranes exhibited reduced enzymatic activity compared to full-thickness skin (65), possibly due to the exposure to heat required to separate epidermal and dermal membranes. Furthermore, the *in vivo* efficacy study will be conducted in female BALB/c mice and thus full-thickness mouse skin was used to assure consistency between the *in vitro* – *in vivo* data set. During the preparation of our homogenate intracellular enzymes might have been released contributing to the breakdown of drugs, in which case these results represent an overestimation of drug metabolism (62). How these results compare to human skin is unclear but a study comparing paraben breakdown in rat and human skin, observed a higher metabolism, in the order of magnitudes, for rat skin indicating that the breakdown in human skin is expected to be lower as compared to the results obtained here (66).

Drug binding to skin proteins can also result in the inability of the drug to reach or distribute to its target; it is the unbound (free) fraction of the drug in the dermis that is pharmacologically active as it can passively permeate into the macrophage and from there into the parasite (67). After incubation in skin homogenate, our test compounds exhibited a range of unbound fractions. A certain level of drug-skin binding is desirable to establish a depot effect leading to slow release of the drug from the skin into the macrophage and *Leishmania* parasite. As the unbound fractions across a membrane are in equilibrium, drug being taken up by the macrophage will cause drug bound to skin components to be released and become available for uptake into the macrophage. Moreover, the skin binding could prevent systemic exposure and therefore preliminary drug metabolism and excretion.

Prior to *in vivo* evaluation, the skin disposition of the compounds was evaluated using BALB/c mouse skin under real-life conditions e.g. limited volume of a 1% (w/v) test compound formulation. This showed a lower permeation for LSH002 compared to LSH001 and LSH003 in contrast to its higher permeation shown in the RHE. This is likely due to the change in vehicle and thus saturation therein. LSH001 and LSH003 were applied as suspensions with a maximal thermodynamic activity, while LSH002 was applied as a solution at about 80% of saturation and thus a suboptimal thermodynamic driving force. Also due to its hydrophilic nature, LSH002 is likely to have a higher affinity for the ethanol-PG vehicle compared to the skin causing the drug to remain in the vehicle on the skin surface. In addition, our mass balance data showed a

AAC

significantly lower drug fraction in the skin for both LSH002 and LSH003 compared to LSH001 (one-way ANOVA; $p<0.05$). For LSH001 about half of the applied drugs had permeated into the skin. LSH001 has a high log D which is expected to facilitate partitioning and diffusion into the stratum corneum. A high log D, however, is unfavourable for the permeation into the dermis.

When evaluating the activity of these test compounds *in vivo*, LSH001 applied topically was able to halt the lesion growth, which suggests that the drug was able to permeate through the SC and reach the parasites situated in the lower epidermis and dermis. LSH003 administered orally, significantly reduced the lesion size and parasite burden compared to the LSH001 and LSH002 oral groups. This non-healing BALB/c model is a rigorous test for drugs because (i) upon infection with *Leishmania* parasites, the mice develop fulminating infections with ulcers that quickly progress to death if left untreated (68), and (ii) the drugs were only applied after establishment of the lesions. For this model lesion size reduction or suppression of lesion growth is regarded as a promising result (68).

The determination of efficacy of the topical formulations can be difficult to gauge as the mice are able to remove the formulation by licking the site. For LSH001, there was no change in lesion progression when the compound was administered orally. This suggests that the drug that permeated the skin exerts the suppression of nodule growth observed upon topical application of the same agent. This correlates with the data obtained from the *in vitro* permeation experiment using BALB/c mouse skin. Not only did LSH001 show a higher permeation compared to LSH002 and LSH003, the mass balance study also showed a statistically higher concentration of LSH001 in the skin compared to the two other test

AAC

compounds. Of the three *in vivo* tested compounds, LSH001 also exhibited the highest unbound fraction. It could be hypothesised that even for topical compounds it is beneficial to have a high unbound fraction in order to exert anti-leishmanial activity as opposed to binding to skin.

LSH001 suppressed nodule growth when applied topically whereas oral administration with the same agent did not affect lesion size and vice versa for LSH003 whereby oral administration reduced the lesion size but topical administration had no effect. Since LSH001 and LSH003, exhibited the same *in vitro* activity against *L. major, i*t is thus suggested that the difference in efficacy upon oral administration is due to pharmacokinetic variations between LSH001 and LSH003.

## ***Conclusions***

Previously, the process of drug development for CL mainly focussed on drug activity testing and formulation optimisation. Current *in vitro* models to test anti-leishmanial activity rely on 2D culture systems that demonstrate activity against the intracellular parasite but correlate poorly with results obtained in animal models (69). This “disconnect” is likely to be caused by the oversimplification of the *in vitro* model that is unable to account for pharmacokinetic drug barriers that occur *in vivo*.

We have shown that a more complete evaluation of a drug candidate is established by incorporating physiologically-based pharmacokinetic assays in our drug discovery, leading to an improved selection of lead candidates, which is essential to improve the likelihood of a success of clinical candidates (70, 71).

Furthermore, this step-wise approach allows evaluation of the test compounds at each stage enables input from medicinal chemistry to alter the core molecule to optimise physicochemical properties to increase distribution and specificity of the drug in the skin at an early stage of development.

## Acknowledgements

This research was supported by funding from the Bloomsbury Colleges London and the Charlotte and Yule Bogue Research Fund from the University College London

## Funding

Each author is, or was, at the time of the work, a paid employee of their affiliated organization. Further this work was financially supported by the Bloomsbury Colleges London and a Bogue fellowship to Katrien Van Bocxlaer.

## Transparency declarations

None to declare

AAC

## *References*

1. **Alvar J, Velez ID, Bern C, Herrero M, Desjeux P, Cano J, Jannin J, den Boer M.** 2012. Leishmaniasis Worldwide and Global Estimates of Its Incidence. PLoS One **7:**e35671.
2. **Desjeux P.** 2001. The increase in risk factors for leishmaniasis worldwide. Transactions of the Royal Society of Tropical Medicine and Hygiene **95**.
3. **Alirol E, Getaz L, Stoll B, Chappuis F, Loutan L.** 2011. Urbanisation and infectious diseases in a globalised world. The Lancet Infectious Diseases **11:**131-141.
4. **Rangel EF, da Costa SM, Carvalho BM.** 2014. Environmental Changes and the Geographic Spreading of American Cutaneous Leishmaniasis in Brazil. *In* Claborn D (ed), Leishmaniasis - Trends in Epidemiology, Diagnosis and Treatment.
5. **Hayani K, Dandashli A, Weisshaar E.** 2014. Cutaneous Leishmaniasis in Syria: Clinical Features, Current Status and the Effects of War. Acta Derm Venereol doi:10.2340/00015555-1988.
6. **Kassi M, Afghan A, Rehman R, Kasi PM.** 2008. Marring leishmaniasis: the stigmatization and the impact of cutaneous leishmaniasis in Pakistan and Afghanistan. Plos Neglected Tropical Diseases **2:**1-3.
7. **Alvar J, Croft S, Olliaro P.** 2006. Chemotherapy in the treatment and control of leishmaniasis. Advances in Parasitology **61:**223-274.
8. **De Rycker M, Hallyburton I, Thomas J, Campbell L, Wyllie S, Joshi D, Cameron S, Gilbert IH, Wyatt PG, Frearson JA, Fairlamb AH, Gray DW.** 2013. Comparison of a high-throughput high-content intracellular Leishmania donovani assay with an axenic amastigote assay. Antimicrob Agents Chemother **57:**2913-2922.
9. **Pena I, Pilar Manzano M, Cantizani J, Kessler A, Alonso-Padilla J, Bardera AI, Alvarez E, Colmenarejo G, Cotillo I, Roquero I, de Dios-Anton F, Barroso V, Rodriguez A, Gray DW, Navarro M, Kumar V, Sherstnev A, Drewry DH, Brown JR, Fiandor JM, Julio Martin J.** 2015. New compound sets identified from high throughput phenotypic screening against three kinetoplastid parasites: an open resource. Sci Rep **5:**8771.
10. **Carneiro G, Aguiar MG, Fernandes AP, Ferreira LA.** 2012. Drug delivery systems for the topical treatment of cutaneous leishmaniasis. Expert Opin Drug Deliv T - aheadofprint.
11. **Frankenburg S, Glick D, Klaus S, Barenholz Y.** 1998. Efficacious topical treatment for murine cutaneous leishmaniasis with ethanolic formulations of amphotericin B. Antimicrob Agent Chemother **42:**3092-3096.
12. **Vardy D, Barenholz Y, Naftoliev N, Klaus S, Gilead L, Frankenburg S.** 2001. Efficacious topical treatment for human cutaneous leishmaniasis with ethanolic lipid amphotericin B. Trans R Soc Trop Med Hyg **95:**184-186.
13. **Hussain A, Samad A, Nazish I, Ahmed FJ.** 2014. Nanocarrier-based topical drug delivery for an antifungal drug. Drug Dev Ind Pharm **40:**527-541.
14. **Ruiz HK, Serrano DR, Dea-Ayuela MA, Bilbao-Ramos PE, Bolas-Fernandez F, Torrado JJ, Molero G.** 2014. New amphotericin B-gamma cyclodextrin formulation for topical use with synergistic activity against diverse fungal species and Leishmania spp. Int J Pharm doi:10.1016/j.ijpharm.2014.07.004.
15. **El-On J, Jacobs GP, Witztum E, Greenblatt CL.** 1984. Development of topical treatment for cutaneous leishmaniasis caused by Leishmania major in experimental animals. Antimicrob Agents Chemother **26:**745-751.
16. **El-On J, Jacobs GP, Weinrauch L.** 1988. Topical chemotherapy of cutaneous Leishmaniasis. Parasitology Today **4:**76-81.
17. **Carter KC, Alexander J, Baillie AJ.** 1989. Studies on the topical treatment of experimental cutaneous leishmaniasis: the therapeutic effect of methyl benzethonium chloride and the

aminoglycosides, gentamicin and paromomycin. Annals of Tropical and Medicine and Parasitology **83:**233-239.

18. **Grogl M, Schuster BG, Ellis WY, Berman JD.** 1999. Successful topical treatment of murine cutaneous leishmaniasis with a combination of paromomycin (Aminosidine) and gentamicin. Journal of Parasitology **85:**354-359.

19. **Ferreira LS, Ramaldes GA, Nunan EA, Ferreira LA.** 2004. In vitro skin permeation and retention of paromomycin from liposomes for topical treatment of cutaneous leishmaniasis. Drug Development and Industrial Pharmacy **30:**289-296.

20. **Van Bocxlaer K, Yardley V, Murdan S, Croft SL.** 2015. Drug permeation and barrier damage in *Leishmania*-infected mouse skin. JAC.

21. **Croft SL, Seifert K, Yardley V.** 2006. Current scenario of drug development for leishmaniasis. Indian Journal of Medical Research **123:**399-410.

22. **Jacobs RT, Plattner JJ, Keenan M.** 2011. Boron-based drugs as antiprotozoals. Current Opinion in Infectious Diseases **24:**586-592.

23. **Zhang YK, Plattner JJ, Freund YR, Easom EE, Zhou Y, Gut J, Rosenthal PJ, Waterson D, Gamo FJ, Angulo-Barturen I, Ge M, Li Z, Li L, Jian Y, Cui H, Wang H, Yang J.** 2011. Synthesis and structure-activity relationships of novel benzoxaboroles as a new class of antimalarial agents. Bioorg Med Chem Lett **21:**644-651.

24. **Zhang YK, Plattner JJ, Freund YR, Easom EE, Zhou Y, Ye L, Zhou H, Waterson D, Gamo FJ, Sanz LM, Ge M, Li Z, Li L, Wang H, Cui H.** 2012. Benzoxaborole antimalarial agents. Part 2: Discovery of fluoro-substituted 7-(2-carboxyethyl)-1,3-dihydro-1-hydroxy-2,1-benzoxaboroles. Bioorg Med Chem Lett **22:**1299-1307.

25. **Jacobs RT, Plattner JJ, Nare B, Wring SA, Chen D, Freund Y, Gaukel EG, Orr MD, Perales JB, Jenks M, Noe RA, Sligar JM, Zhang YK, Bacchi CJ, Yarlett N, Don R.** 2011. Benzoxaboroles: a new class of potential drugs for human African trypanosomiasis. Future Medicinal Chemistry **3:**1259-1278.

26. **Hu Q-H, Liu R-J, Fang Z-P, Zhang J, Ding Y-Y, Tan M, Wang M, Pan W, Zhou H-C, Wang E-D.** 2013. Discovery of a potent benzoxaborole-based anti-pneumococcal agent targeting leucyl-tRNA synthetase. Sci Rep **3**.

27. **Liu CT, Tomsho JW, Benkovic SJ.** 2014. The unique chemistry of benzoxaboroles: Current and emerging applications in biotechnology and therapeutic treatments. Bioorganic & Medicinal Chemistry **22:**4462-4473.

28. **Nare B, Wring S, Bacchi C, Beaudet B, Bowling T, Brun R, Chen D, Ding C, Freund Y, Gaukel E, Hussain A, Jarnagin K, Jenks M, Kaiser M, Mercer L, Mejia E, Noe A, Orr M, Parham R, Plattner J, Randolph R, Rattendi D, Rewerts C, Sligar J, Yarlett N, Don R, Jacobs R.** 2010. Discovery of novel orally bioavailable oxaborole 6-carboxamides that demonstrate cure in a murine model of late-stage central nervous system african trypanosomiasis. Antimicrobial Agents and Chemotherapy **54:**4379-4388.

29. **Edwards JE, Brouwer KR, McNamara PJ.** 2002. GF120918, a P-glycoprotein modulator, increases the concentration of unbound amprenavir in the central nervous system in rats. Antimicrob Agents Chemother **46:**2284-2286.

30. **Troutman MD, Thakker DR.** 2003. Novel experimental parameters to quantify the modulation of absorptive and secretory transport of compounds by P-glycoprotein in cell culture models of intestinal epithelium. Pharmaceutical Research **20:**1210-1224.

31. **Thiel-Demby VE, Tippin TK, Humphreys JE, Serabjit-Singh CJ, Polli JW.** 2004. In vitro absorption and secretory quotients: practical criteria derived from a study of 331 compounds to assess for the impact of P-glycoprotein-mediated efflux on drug candidates. Journal of Pharmaceutical Sciences **93:**2567-2572.

AAC

32. **Thiel-Demby VE, Humphreys JE, St John Williams LA, Ellens HM, Shah N, Ayrton AD, Polli JW.** 2009. Biopharmaceutics classification system: validation and learnings of an in vitro permeability assay. Mol Pharm **6:**11-18.

33. **Mahjour M, Mauser BE, Rashidbaigi ZA, Fawzi MB.** 1993. Effects of propylene glycol diesters of caprylic and capric acids (Miglyol® 840) and ethanol binary systems on in vitro skin permeation of drugs. International Journal of Pharmaceutics **95:**161-169.

34. **van der Meide W, Guerra J, Schoone G, Farenhorst M, Coelho L, Faber W, Peekel I, Schallig H.** 2008. Comparison between quantitative nucleic acid sequence-based amplification, real-time reverse transcriptase PCR, and real-time PCR for quantification of Leishmania parasites. Journal of Clinical Microbiology **46:**73-78.

35. **Irvine JD, Takahashi L, Lockhart K, Cheong J, Tolan JW, Selick HE, Grove JR.** 1999. MDCK (Madin-Darby Canine Kidney) Cells: A Tool for Membrane Permeability Screening. Journal of Pharmaceutical Sciences **88:**28-33.

36. **Costa IS, de Souza GF, de Oliveira MG, Abrahamsohn Ide A.** 2013. S-nitrosoglutathione (GSNO) is cytotoxic to intracellular amastigotes and promotes healing of topically treated Leishmania major or Leishmania braziliensis skin lesions. J Antimicrob Chemother **68:**2561-2568.

37. **initiative D-DfND.** 2016. DNDi portfolio June 2016, *on* DNDi - Drugs for Neglected Diseases initiative. http://www.dndi.org/diseases-projects/portfolio/. Accessed 15-03-2017.

38. **Bos JD, Meinardi MM.** 2000. The 500 Dalton rule for the skin penetration of chemical compounds and drugs. Exp Dermatol **9:**165-169.

39. **Hadgraft J, Pugh WJ.** 1998. The selection and design of topical and transdermal agents: a review. Journal of Investigative Dermatology: Symposium Proceeding **3:**131-135.

40. **Choy YB, Prausnitz MR.** 2011. The rule of five for non-oral routes of drug delivery: ophthalmic, inhalation and transdermal. Pharm Res **28:**943-948.

41. **Vecchia BE, Bunge AL.** 2002. Evaluating the Transdermal Permeability of Chemicals, Transdermal Drug Delivery Systems doi:doi:10.1201/9780203909683.ch210.1201/9780203909683.ch2. CRC Press.

42. **Naik A, Kalia YN, Guy RH.** 2000. Transdermal drug delivery: overcoming the skin's barrier function. Pharmaceutical Science and Technology Today **3:**318-326.

43. **Roberts MS, Pugh WJ, Hadgraft J.** 1996. Epidermal permeability: Penetrant structure relationships .2. The effect of H-bonding groups in penetrants on their diffusion through the stratum corneum. International Journal of Pharmaceutics **132:**23-32.

44. **Brody I.** 1977. Ultrastructure of the stratum corneum. International Journal of Dermatology **16:**245-256.

45. **Downing DT, Stewart ME, Wertz PW, Colton SW, Strauss JS.** 1983. Skin lipids. Comparative Biochemistry and Physiology B **76:**673-678.

46. **Neal RA, Croft SL.** 1984. An in-vitro system for determining the activity of compounds against the intracellular amastigote form of Leishmania donovani. J Antimicrob Chemother **14:**463-475.

47. **Mahar Doan KM, Wring SA, Shampine LJ, Jordan KH, Bishop JP, Kratz J, Yang E, Serabjit-Singh CJ, Adkison KK, Polli JW.** 2004. Steady-state brain concentrations of antihistamines in rats: interplay of membrane permeability, P-glycoprotein efflux and plasma protein binding. Pharmacology **72:**92-98.

48. **Evers R, Kool M, Smith AJ, van Deemter L, de Haas M, Borst P.** 2000. Inhibitory effect of the reversal agents V-104, GF120918 and Pluronic L61 on MDR1 Pgp-, MRP1- and MRP2-mediated transport. Br J Cancer **83:**366-374.

49. **Tran TT, Mittal A, Aldinger T, Polli JW, Ayrton A, Ellens H, Bentz J.** 2005. The elementary mass action rate constants of P-gp transport for a confluent monolayer of MDCKII-hMDR1 cells. Biophys J **88:**715-738.

50. **Acharya P, O'Connor MP, Polli JW, Ayrton A, Ellens H, Bentz J.** 2008. Kinetic identification of membrane transporters that assist P-glycoprotein-mediated transport of digoxin and loperamide through a confluent monolayer of MDCKII-hMDR1 cells. Drug Metab Dispos **36:**452-460.

51. **Janneh O, Jones E, Chandler B, Owen A, Khoo SH.** 2007. Inhibition of P-glycoprotein and multidrug resistance-associated proteins modulates the intracellular concentration of lopinavir in cultured CD4 T cells and primary human lymphocytes. J Antimicrob Chemother **60:**987-993.

52. **Jovelet C, Deroussent A, Broutin S, Paci A, Farinotti R, Bidart JM, Gil S.** 2013. Influence of the multidrug transporter P-glycoprotein on the intracellular pharmacokinetics of vandetanib. Eur J Drug Metab Pharmacokinet **38:**149-157.

53. **Lemaire S, Van Bambeke F, Mingeot-Leclercq MP, Tulkens PM.** 2007. Modulation of the cellular accumulation and intracellular activity of daptomycin towards phagocytized Staphylococcus aureus by the P-glycoprotein (MDR1) efflux transporter in human THP-1 macrophages and madin-darby canine kidney cells. Antimicrob Agents Chemother **51:**2748-2757.

54. **Seral C, Carryn S, Tulkens PM, Van Bambeke F.** 2003. Influence of P-glycoprotein and MRP efflux pump inhibitors on the intracellular activity of azithromycin and ciprofloxacin in macrophages infected by Listeria monocytogenes or Staphylococcus aureus. J Antimicrob Chemother **51:**1167-1173.

55. **Mookerjee Basu J, Mookerjee A, Banerjee R, Saha M, Singh S, Naskar K, Tripathy G, Sinha PK, Pandey K, Sundar S, Bimal S, Das PK, Choudhuri SK, Roy S.** 2008. Inhibition of ABC transporters abolishes antimony resistance in Leishmania Infection. Antimicrob Agents Chemother **52:**1080-1093.

56. **Alvarez-Figueroa MJ, Pessoa-Mahana CD, Palavecino-Gonzalez ME, Mella-Raipan J, Espinosa-Bustos C, Lagos-Munoz ME.** 2011. Evaluation of the membrane permeability (PAMPA and skin) of benzimidazoles with potential cannabinoid activity and their relation with the Biopharmaceutics Classification System (BCS). AAPS PharmSciTech **12:**573-578.

57. **Schreiber S, Mahmoud A, Vuia A, Rubbelke MK, Schmidt E, Schaller A, Kandarova H, Haberland A, Schafer UF, Bock U, Korting HC, Liebsch A, Schafer-Korting A.** 2005. Reconstructed epidermis versus human and animal skin in skin absorption studies. Toxicology in Vitro **19:**813-822.

58. **Schafer-Korting M, Bock U, Gamer A, Haberland A, Haltner-Ukomadu E, Kaca M, Kamp H, Kietzmann M, Korting HC, Krachter HU, Lehr CM, Liebsch M, Mehling A, Netzlaff F, Niedorf F, Rubbelke MK, Schafer U, Schmidt E, Schreiber S, Schroder KR, Spielmann H, Vuia A.** 2006. Reconstructed human epidermis for skin absorption testing: results of the German prevalidation study. Altern Lab Anim **34:**283-294.

59. **Lotte C, Patouillet C, Zanini M, Messager A, Roguet R.** 2002. Permeation and Skin Absorption: Reproducibility of Various Industrial Reconstructed Human Skin Models. Skin Pharmacology and Physiology **15(suppl 1):**18-30.

60. **Kao J, Patterson FK, Hall J.** 1985. Skin penetration and metabolism of topically applied chemicals in six mammalian species, including man: an in vitro study with benzo[a]pyrene and testosterone. Toxicology and Applied Pharmacology **81:**502-516.

61. **Muller B, Kasper M, Surber C, Imanidis G.** 2003. Permeation, metabolism and site of action concentration of nicotinic acid derivatives in human skin. Correlation with topical pharmacological effect. Eur J Pharm Sci **20:**181-195.

62. **Morris AP, Brain KR, Heard CM.** 2009. Skin permeation and ex vivo skin metabolism of O-acyl haloperidol ester prodrugs. Int J Pharm **367:**44-50.

63. **Montagna W.** 1955. Histology and cytochemistry of human skin: IX. The distribution of non-specific esterases The Journal of Biophysical and Biochemical Cytology **1:**13-16.

AAC

64. **Ozaki H, Sugihara K, Watanabe Y, Fujino C, Uramaru N, Sone T, Ohta S, Kitamura S.** 2013. Comparative study of the hydrolytic metabolism of methyl-, ethyl-, propyl-, butyl-, heptyl- and dodecylparaben by microsomes of various rat and human tissues. Xenobiotica **43:**1064-1072.

65. **Bonina FP, Puglia C, Barbuzzi T, de Caprariis P, Palagiano F, Rimoli MG, Saija A.** 2001. In vitro and in vivo evaluation of polyoxyethylene esters as dermal prodrugs of ketoprofen, naproxen and diclofenac. European Journal of Pharmaceutical Sciences **14:**123-134.

66. **Harville HM, Voorman R, Prusakiewicz JJ.** 2007. Comparison of paraben stability in human and rat skin. Drug Metab Lett **1:**17-21.

67. **Gonzalez D, Schmidt S, Derendorf H.** 2013. Importance of relating efficacy measures to unbound drug concentrations for anti-infective agents. Clin Microbiol Rev **26:**274-288.

68. **Yardley V, Croft SL.** 1999. Animal Models of Cutaneous Leishmaniasis, p 775-781. *In* Zak O (ed), Handbook of Animals of Infection. Academic Press London.

69. **Coelho AC, Trinconi CT, Costa CH, Uliana SR.** 2014. In vitro and in vivo miltefosine susceptibility of a Leishmania amazonensis isolate from a patient with diffuse cutaneous leishmaniasis. PLoS Negl Trop Dis **8:**e2999.

70. **Katsuno K, Burrows JN, Duncan K, Hooft van Huijsduijnen R, Kaneko T, Kita K, Mowbray CE, Schmatz D, Warner P, Slingsby BT.** 2015. Hit and lead criteria in drug discovery for infectious diseases of the developing world. Nat Rev Drug Discov **14:**751-758.

71. **Grogl M, Hickman M, Ellis W, Hudson T, Lazo JS, Sharlow ER, Johnson J, Berman J, Sciotti RJ.** 2013. Drug discovery algorithm for cutaneous leishmaniasis. Am J Trop Med Hyg **88:**216-221.

## Tables

Table 1. The general structure of benzoxaboroles (A) and subclasses: benzoxaborole 6-carboxamides (D), benzoxaboroles 5-carboxamides (B), pyrazole 6-carboxamides (C), benzoxaborininols (E).

**General benzoxaboroles structure**

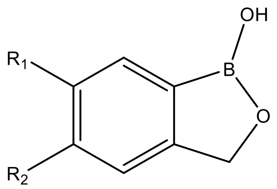

| Chemical sub class |  | Modification | Compound ID |
|---|---|---|---|
| Benzoxaborole 6-carboxamide | **R1** | 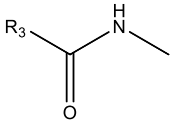 | **LSH006, LSH009, LSH010, LSH011, LSH012, LSH015, LSH016, LSH019, LSH020, LSH021, LSH023, LSH024, LSH025** |
| Benzoxaborole 5-carboxamide | **R2** | 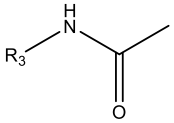 | **LSH002, LSH031** |
| Pyrazole 6-carboxamides | **R1** | 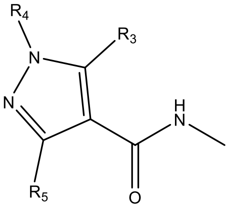 | **LSH022, LSH027, LSH028, LSH029** |
| benzoxaborininole |  | 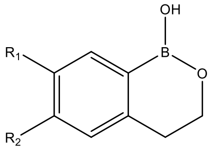 | **LSH001, LSH033** |
| Other |  |  | **LSH004, LSH005, LSH007, LSH013, LSH017,LSH018, LSH034** |

Table 2. Summary of the experimental conditions for the different permeation experiments.

| Permeation experiment | Compounds | Donor vehicle | Concentration (µg/ml) | Volume/ skin surface (µl/cm$^2$) |
|---|---|---|---|---|
| **RHE 1** | LSH001; LSH003; LSH011; LSH012; LSH023; LSH024; LSH029; LSH034; caffeine; testosterone | Ethanol – Miglyol 840 (1:9)<br>Except for caffeine | 100 | 300 |
| **FDC 1** | Mix1: LSH001; LSH002<br>Mix2: LSH003; LSH034 | Ethanol – Miglyol 840 (1:9) | 100 | 300 |
| **FDC 2** | LSH001;<br>LSH002; LSH003 | Ethanol – PG (1:1) | 10 000<br>(1% w/v) | 28.4 |

Table 3. Summary of the different *in vivo* experimental groups with their treatment regimen.

| Group | Formulation | Active compound | Vehicle | Administration route | Treatment regimen |
|---|---|---|---|---|---|
| **1** | Untreated control | None | None | None | None |
| **2** | AmBisome® | Amphotericin B | Dextrose 5% | IV | 25mg/kg/b.i.d, 5 doses |
| **3** | Leshcutan® | Paromomycin sulphate 15% | Methylbenzethonium chloride 12% in vaseline | Topical | 0.1ml 2/day for 10 days |
| **4** | Vehicle control | N/A | PG/Ethanol (1:1) | Topical | 2x50µl/day for 10 days |
| **5** | Topical formulation 1 | LSH001 | Saturated drug solution in PG/Ethanol (1:1) | Topical | 2x50µl/day for 10 days |
| **6** | Topical formulation 2 | LSH002 | | | |
| **7** | Topical formulation 3 | LSH003 | | | |
| **8** | Oral formulation 1 | LSH001 | Standard suspended vehicle | Oral | 2x25mg/kg/day for 10 days |
| **9** | Oral formulation 2 | LSH002 | | | |
| **10** | Oral formulation 3 | LSH003 | | | |

AAC

Table 4. The sequences of the primer and probes used in the PCR and qPCR reactions.

| | Gene | Primer/probe | Primer Sequence |
|---|---|---|---|
| ***Leishmania* species** | 18S rDNA (170-bp) | Forward primer | 5'-C CAA AGT GTG GAG ATC GAA G-3' |
| | | Reverse primer | 5'-GGC CGG TAA AGG CCG AAT AG-3' |
| | | Probe | 5'-6FAM ACCATTGTAGTCCACACTGC-NFQ-MGB |

Table 5. Activity of benzoxaborole compounds against intracellular *Leishmania* amastigotes ($EC_{50}$ values (µM) and 95% CI, n=number of experiment repeats).

| Compound | n | *L. tropica* | *L. major* | *L. aethiopica* | *L. mexicana* | *L. panamensis* |
|---|---|---|---|---|---|---|
| **Amphotericin B** | 1 | 0.066<br>(0.062-0.070) | 0.043<br>(0.037-0.049) | 0.115<br>(0.107-0.122) | 0.430<br>(0.394-0.460) | 0.143<br>(0.131-0.156) |
| | 2 | 0.083<br>(0.078-0.089) | 0.049<br>(0.043-0.056) | 0.107<br>(0.096-0.119) | 0.685<br>(0.553-0.692) | 0.115<br>(0.093-0.142) |
| **Miltefosine** | 1 | 19.99<br>(17.40-22.97) | 44.85<br>(22.02-77.28) | 7.79<br>(6.20-9.78) | 31.04<br>(28.56-33.73) | 19.98<br>(16.17-24.69) |
| | 2 | 9.44<br>(7.78-11.45) | 26.58<br>(21.30-33.15) | 7.95<br>(7.26-8.69) | 45.86<br>(36.61-57.45) | 23.11<br>(20.41-26.18) |
| **LSH001** | 1 | 2.01<br>(1.52-2.67) | 4.26<br>(2.97-6.11) | 22.10<br>(15.07-32.41) | 23.04<br>(15.99-33.19) | 18.82<br>(14.08-25.14) |
| | 2 | 3.12<br>(2.38-4.09)) | 7.61<br>(5.48-10.57) | 26.83<br>(19.40-37.11) | 16.94<br>(9.62-29.83) | 13.96<br>(10.06-19.44) |
| **LSH002** | 1 | 14.96<br>(11.38-19.67) | 16.52<br>(11.56-23.61) | > 30 | > 30 | > 30 |
| **LSH003** | 1 | 2.46<br>(1.78-3.41) | 3.93<br>(3.32-4.64) | 11.12<br>(7.67-16.13) | 18.94<br>(10.78-33.29) | 8.09<br>(6.56-9.96) |
| | 2 | 3.94<br>(2.96-5.25)) | 3.10<br>(2.25-4.26)) | > 30 | > 30 | 19.05<br>(15.03-24.16) |
| **LSH004** | 1 | 16.08<br>(13.70-18.80) | - | 29.97<br>(19.04-47.16) | > 30 | > 30 |
| **LSH005** | 1 | 6.81<br>(5.84-7.94) | - | 21.25<br>(13.18-34.26) | > 30 | > 30 |
| **LSH006** | 1 | > 30 | - | 25.36<br>(15.88-40.50) | > 30 | > 30 |
| **LSH007** | 1 | 5.71<br>(4.39-7.43) | - | 27.18<br>(17.16-43.04) | > 30 | > 30 |
| **LSH008** | 1 | > 30 | - | > 30 | > 30 | > 30 |
| **LSH009** | 1 | 3.08<br>(2.51-3.79) | - | 17.66<br>(12.10-25.76) | > 30 | > 30 |
| **LSH010** | 1 | 6.23<br>(5.49-7.06) | > 30 | 11.71<br>(7.22-19.00) | > 30 | > 30 |
| **LSH011** | 1 | 2.31<br>(1.73-3.08) | 9.92<br>(8.49-11.59) | > 30 | > 30 | > 30 |
| **LSH012** | 1 | 24.61 | 9.52 | > 30 | > 30 | > 30 |

AAC

| | | | | | | |
|---|---|---|---|---|---|---|
| | | (14.31-42.30) | (6.80-13.32) | | | |
| **LSH013** | 1 | > 30* | > 30 | > 30 | > 30 | > 30 |
| **LSH014** | 1 | 5.91* (4.63-7.54) | 4.15 (3.42-5.04) | > 30 | > 30 | 29.59 (20.59-42.53) |
| **LSH015** | 1 | 6.92 (4.95-9.66) | > 30 | > 30 | > 30 | > 30 |
| **LSH016** | 1 | 5.40 (4.02-7.26) | > 30 | 21.84 (14.60-32.66) | > 30 | > 30 |
| **LSH017** | 1 | > 30 | > 30 | > 30 | > 30 | > 30 |
| **LSH018** | 1 | > 30 | > 30 | > 30 | > 30 | > 30 |
| **LSH019** | 1 | 21.01 (4.07-108.4) | > 30 | > 30 | > 30 | > 30 |
| **LSH020** | 1 | > 30 | > 30 | > 30 | > 30 | > 30 |
| **LSH021** | 1 | 28.81 (17.03-48.74) | > 30 | > 30 | > 30 | > 30 |
| **LSH022** | 1 | > 30 | > 30 | > 30 | > 30 | > 30 |
| **LSH023** | 1 | 1.19* (0.78-1.80) | 1.57 (1.17-2.10) | 23.05 (10.09-52.62) | 6.31 (4.18-9.54) | 2.98 (2.28-3.90) |
| **LSH024** | 1 | 4.72* (3.31-6.74) | 13.96 (11.52-16.91) | > 30 | > 30 | 22.34 (17.66-28.25) |
| **LSH025** | 1 | 2.21* (1.51-3.25) | 5.93 (5.08-6.92) | > 30 | 25.39 (15.81-40.78) | 15.85 (12.85-19.56) |

Table 6. Physicochemical properties of benzoxaborole compounds.

| **Compound** | **Molecular weight* (g/mol)** | **H bond donor/acceptor*** | **Aqueous solubility* (µg/ml)** | **Log D (pH 7.4)**** |
|---|---|---|---|---|
| **Ideal skin permeant** | < 500 | < 3 | | 1-3 |
| **LSH001** | 387 | 2/5 | 9 | > 2.63 |
| **LSH002** | 421 | 2/5 | 37 | 0.44±0.06 |
| **LSH003** | 321 | 2/7 | 165 | 2.18±0.08 |
| **LSH023** | 334 | 2/5 | 103 | 2.45±0.04 |
| **LSH024** | 368 | 2/6 | 45 | 2.16±0.07 |
| **LSH026** | 306 | 2/4 | 22 | 1.86±0.07 |
| **LSH027** | 325 | 2/8 | 103 | 1.53*** |
| **LSH028** | 334 | 2/6 | 53 | 1.86±0.02 |
| **LSH029** | 393 | 2/11 | 14 | 1.95±0.10 |
| **LSH030** | 373 | 2/5 | 13 | 1.94±0.06 |
| **LSH032** | 386 | 2/5 | 11 | 0.88±0.15 |
| **LSH033** | 400 | 2/5 | 7 | 1.70±0.15 |

* Data obtained using ChemBio 3D Ultra 13.0 modeling software

** Experimental data, Mean±SD, n=3

*** Experimental data, n=1

Table 7. The $P_{app}$ values with and without GF918 and the absorptive quotient (AQ) for the MDCK-MDR1 assay.

| Compound | $P_{app}$(nm/s) | $P_{app\ +GF918}$ (nm/s) | AQ |
|---|---|---|---|
| Amprenavir | 58.3 | 378 | 0.846 |
| Propranolol | 395 | 441 | 0.104 |
| LSH001 | 583 | 599 | 0.027 |
| LSH002 | 16.5 | 32.5 | 0.492 |
| LSH003 | 626 | 635 | 0.014 |
| LSH023 | 605 | 593 | -0.020 |
| LSH024 | 236 | 314 | 0.248 |
| LSH025 | 322 | 349 | 0.077 |
| LSH026 | 652 | 655 | 0.005 |
| LSH027 | 209 | 247 | 0.154 |
| LSH028 | 397 | 424 | 0.064 |
| LSH029 | 229 | 268 | 0.146 |
| LSH030 | 436 | 524 | 0.168 |
| LSH032 | 232 | 327 | 0.291 |
| LSH033 | 404 | 482 | 0.162 |
| LSH034 | 543 | 538 | -0.009 |

Table 8. Fractions of unbound compound and remaining compound after 2 hours incubation with mouse skin supernatant (protein content 2.5 mg/ml).

| Compound | % unbound | % remaining test compound |
|---|---|---|
| **ethyl paraben** | | 10.9 |
| **propyl paraben** | | 0.0 |
| **LSH001** | 87 | 44.1 |
| **LSH002** | 59 | 28.0 |
| **LSH003** | 44 | 51.0 |
| **LSH023** | 34 | 50.2 |
| **LSH024** | 50 | 35.0 |
| **LSH025** | 66 | 34.3 |
| **LSH026** | 92 | 50.8 |
| **LSH027** | 62 | 53.8 |
| **LSH028** | 60 | 41.5 |
| **LSH029** | 79 | 64.2 |
| **LSH030** | 67 | 46.2 |
| **LSH032** | 57 | 41.7 |
| **LSH033** | 65 | 46.3 |

AAC

Table 9. The permeation parameters: flux and lag time when using RHE and BALB/c mouse skin under same conditions and BALB/c mouse skin when applying a low volume (mean±sd; n=3 except for * where n=2).

| | RHE | BALB/c | BALB/c Low volume |
|---|---|---|---|
| **Testosterone** | | | |
| flux (ng/cm$^2$/h) | 28.0±0.8 | 2.2±0.8 | |
| lag time (h) | 0.7±0.1 | 1.1±0.6 | |
| **LSH001** | | | |
| flux (ng/cm$^2$/h) | 21.8±0.1 | 6.6±0.3* | 88.7±8.8 |
| lag time (h) | 2.2±0.1 | 2.4±0.4 | 2.7±0.5* |
| **LSH002** | | | |
| flux (ng/cm$^2$/h) | 143.9±44.2 | 35.8±0.9* | 13.5±8.7* |
| lag time (h) | 1.7±0.8 | 2.8±0.3 | 2.7±0.7 |
| **LSH003** | | | |
| flux (ng/cm$^2$/h) | 45.1±5.9 | 8.0±1.5* | 71.8±18.0 |
| lag time (h) | 2.1±0.1 | 2.5±0.3 | 2.7±0.9 |

## Figure Legends

**Figure 1. Drug delivery for CL. (A) Progression pathway during lead optimization of drugs as potential topical treatment for CL. (B) Histology of BALB/c mouse skin infected with L. major.** (A) Schematic of the route of the active drug through *Leishmania* infected BALB/c mouse skin before reaching (B) the *Leishmania* amastigotes situated in phagolysosome of dermal macrophages.

**Figure 2. *In vitro* stability of test compounds in skin homogenate.** The remaining fraction (%) of test compound left in supernatant with a protein content of 2.5mg/ml as a function of time (mean±SD, n=3)

**Figure 3. In vitro permeation through BALB/c mouse skin.** The cumulative amount permeated in time for LSH001, LSH002 and LSH003 using Franz diffusion cells (mean±SD, n=3).

**Figure 4. Skin disposition evaluation.** The amounts of benzoxaboroles that permeated or were found in and on the skin expressed as percentage of the dosage retrieved.

**Figure 5. *In vivo* anti-leishmanial activity of benzoxaboroles upon oral and topical application.** (A) The progression of the main lesion size (measured using digital callipers) per group in function of time post infection (n=6, mean±SD); (B) The average number of amastigotes found per lesion as analysed by qPCR and the average lesion size per group 3 days after the end of the treatment (mean±SD, n=5).

AAC

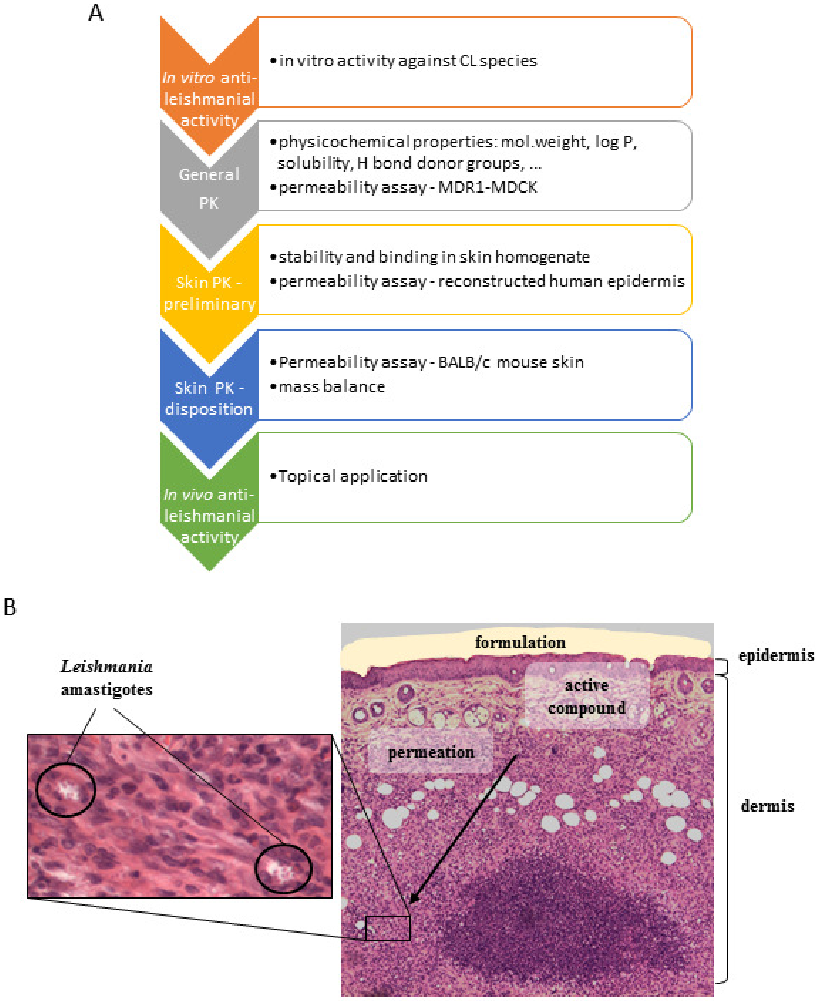
A
*In vitro* anti-leishmanial activity
•in vitro activity against CL species
General PK
•physicochemical properties: mol.weight, log P, solubility, H bond donor groups, ...
•permeability assay - MDR1-MDCK
Skin PK - preliminary
•stability and binding in skin homogenate
•permeability assay - reconstructed human epidermis
Skin PK - disposition
•Permeability assay - BALB/c mouse skin
•mass balance
*In vivo* anti-leishmanial activity
•Topical application
B
*Leishmania* amastigotes
formulation
active compound
permeation
epidermis
dermis

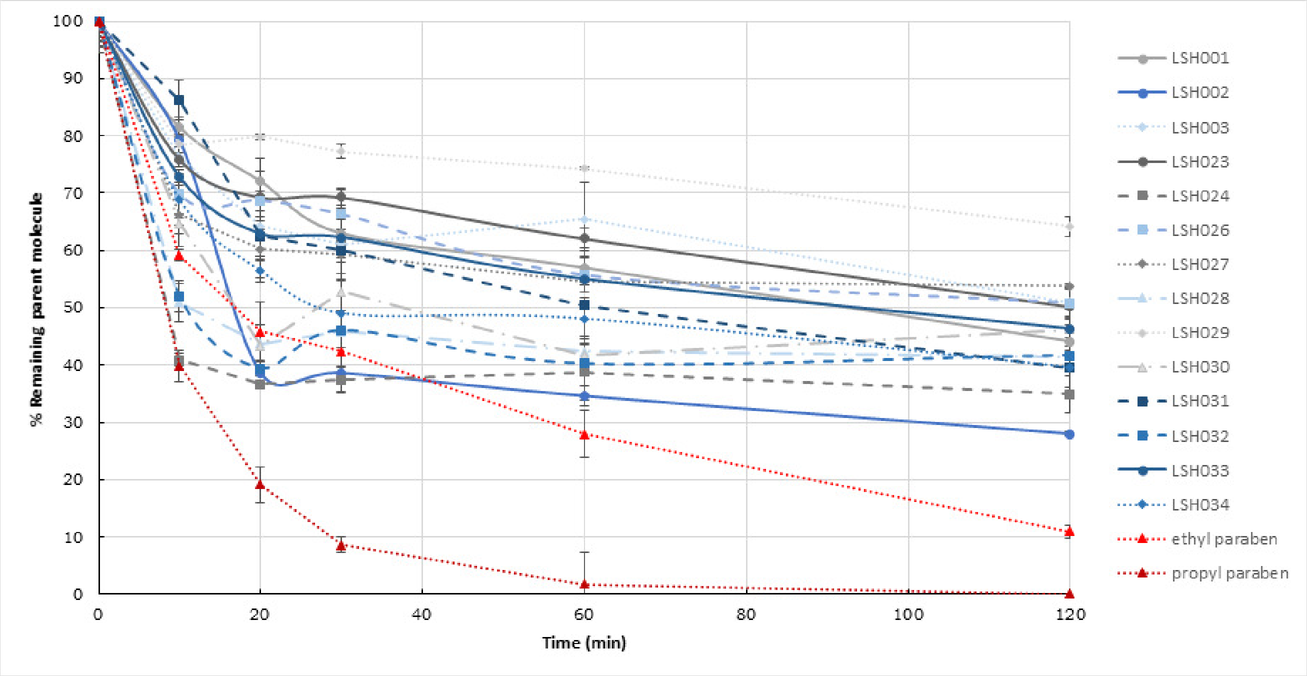
% Remaining parent molecule
100
90
80
70
60
50
40
30
20
10
0
0
20
40
60
80
100
120
Time (min)
LSH001
LSH002
LSH003
LSH023
LSH024
LSH026
LSH027
LSH028
LSH029
LSH030
LSH031
LSH032
LSH033
LSH034
ethyl paraben
propyl paraben

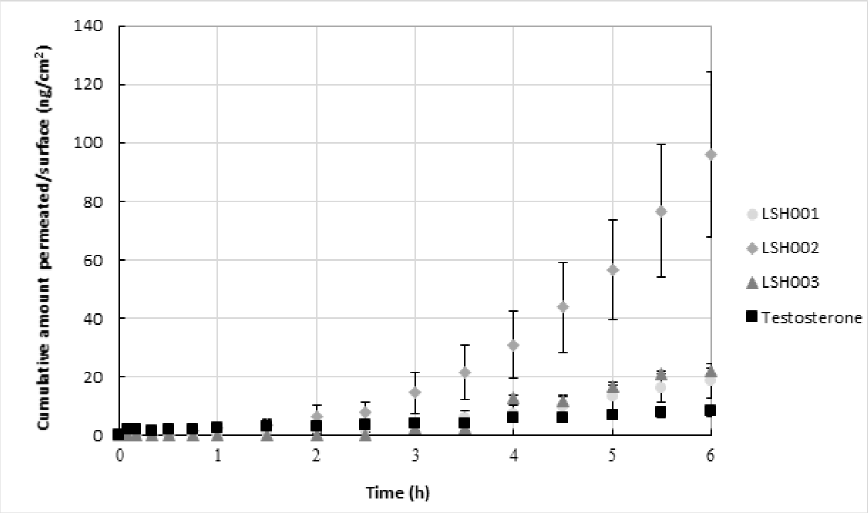
Cumulative amount permeated/surface (ng/cm²)
140
120
100
80
60
40
20
0
0
1
2
3
4
5
6
Time (h)
● LSH001
◆ LSH002
▲ LSH003
■ Testosterone

AAC

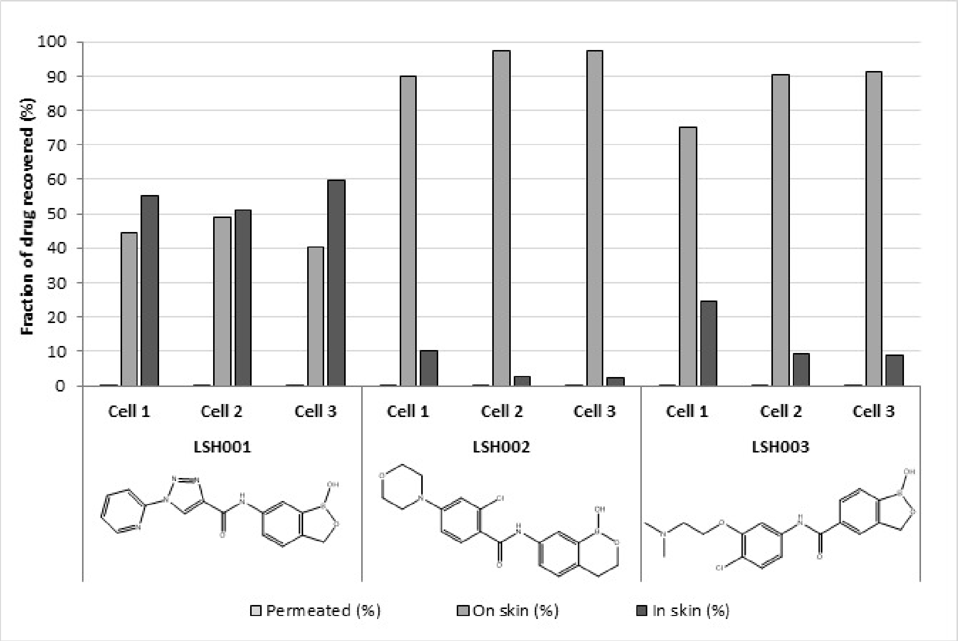
100
90
80
70
60
50
40
30
20
10
0
Fraction of drug recovered (%)
Cell 1
Cell 2
Cell 3
Cell 1
Cell 2
Cell 3
Cell 1
Cell 2
Cell 3
LSH001
LSH002
LSH003
☐ Permeated (%)
▨ On skin (%)
■ In skin (%)

AAC

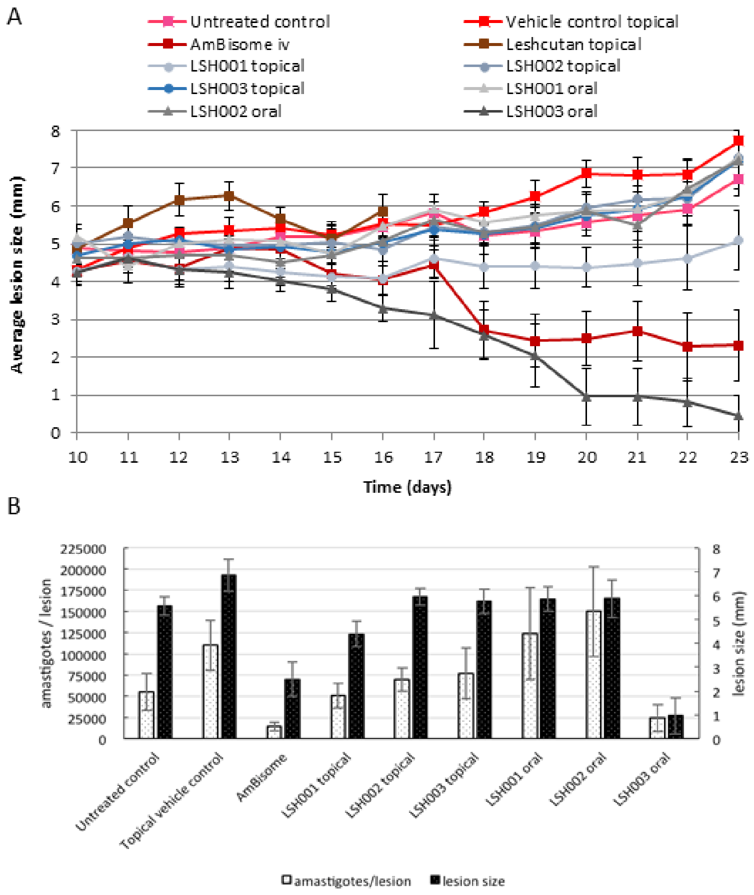
A
Untreated control
Vehicle control topical
AmBisome iv
Leshcutan topical
LSH001 topical
LSH002 topical
LSH003 topical
LSH001 oral
LSH002 oral
LSH003 oral
Average lesion size (mm)
0
1
2
3
4
5
6
7
8
10
11
12
13
14
15
16
17
18
19
20
21
22
23
Time (days)
B
amastigotes / lesion
0
25000
50000
75000
100000
125000
150000
175000
200000
225000
lesion size (mm)
0
1
2
3
4
5
6
7
8
Untreated control
Topical vehicle control
AmBisome
LSH001 topical
LSH002 topical
LSH003 topical
LSH001 oral
LSH002 oral
LSH003 oral
amastigotes/lesion
lesion size